Nuclear Instruments and Methods 171 (1980) 503–519

A "NUCLEAR-SPIN SPECTROMETER": THEORY AND GENERAL CHARACTERISTICS OF A 4π GAMMA-RAY MULTIDETECTOR SYSTEM FOR INVESTIGATIONS OF NUCLEAR STRUCTURE AND REACTIONS AT HIGH ANGULAR MOMENTUM *

D.G. SARANTITES, R. LOVETT and R. WOODWARD
Department of Chemistry, Washington University, St. Louis, Missouri 63130, USA

Received 4 October 1979

The theory and properties of a new type of spectrometer for studying the properties of high-spin states in nuclei and the mechanisms of heavy-ion induced nuclear reactions are presented in some detail. The spectrometer consists of a high efficiency 4π NaI multidetector system with individual tightly packed detector elements. This instrument is capable of recording on an event-by-event basis: (a) the γ-ray multiplicity; (b) the pulse heights and under certain conditions the energies of individual γ-transitions; (c) the total pulse height and the associated γ-ray multiplicity; (d) the associated neutron multiplicity; (e) the angular correlations among most of the γ-rays in the cascade; and (f) the time correlations among the various groups of γ-rays in each cascade. This information is obtained simultaneously thus permitting many correlations to be made among several relevant physical parameters that will enable us to learn more about the properties of nuclei at high-spin and about the role of angular momentum on the mechanism of many types of nuclear reaction.

1. Introduction

A promising tool in investigations of the mechanisms of heavy-ion induced reactions and of the properties of nuclei at very high angular momentum depends upon the suitable detection of the associated electromagnetic radiation. In such investigations two nuclear quantities play the key role. These are the excitation energy and the angular momentum. With the exception of Coulomb excitation and perhaps the few nucleon transfer reactions, most of the reactions currently under investigation involve emission of many particles and γ-rays. Consequently, complete determination of the reaction parameters would require a high order coincidence with a detection system approaching a 4π efficiency. Unlike energy, the angular momenta involved in such interactions cannot be directly observed and are inferred only indirectly. In the majority of heavy-ion collisions a large fraction of the incoming orbital angular momentum is transferred to the main reaction products as intrinsic angular momentum. A more direct determination of the transferred angular momentum on an event-by-event basis can provide many new unique measurements that can increase substantially our understanding of the complex interactions involved.

In this paper we give the theory and expected performance of a class of such 4π multidetector spectrometers capable of providing this information. The detailed performance of one of these spectrometers, currently under construction, will be given in detail in a forthcoming communication. Up to now much of the information about the transferred angular momentum in heavy-ion collisions has been obtained from γ-ray multiplicity measurements [1–6]. In the decay of highly excited high-spin states of equilibrated compound nuclei, most of the excitation energy above the yrast line and only a small fraction of the initial angular momentum is removed by nucleon emission. The remainder of the excitation energy ($\leqslant$50 MeV) and the angular momentum ($\leqslant 70\,\hbar$) is removed by γ-ray emission [2]. For lighter nuclei α-particle emission is also probable and can remove significant amounts of energy and angular momentum. For product nuclei that are deformed most of the angular momentum is known [7–11] to be removed by stretched ($\Delta J = -2$) E2 transitions with a few stretched dipole transitions contributing through complicated cascades along many near parallel collective bands. For product nuclei near

* Work supported in part by the U.S. Department of Energy, Division of Basic Energy Sciences.

closed shells most of the angular momentum has been assumed to be removed [12] by about an equal number of stretched E2 and dipole transitions on the yrast line. Thus, for a given de-excitation path or for a collection of paths, there is a linear relationship between $\langle M_\gamma \rangle$, the multiplicity of the cascades, and the average angular momentum change $\langle \Delta J_\gamma \rangle$ in the cascade. By analogy with the averages, knowledge of M_γ for a given cascade gives a good estimate of the initial angular momentum J_γ from where the cascade started. In such a case, a spectrometer capable of providing M_γ on an event-by-event basis can be named a "spin spectrometer" since it can associate with each event a value of the transferred angular momentum. In previous measurements of the γ-ray multiplicity and the associated few higher moments of the γ-ray multiplicity distribution, use was made of arrangements with 7 to 16 NaI detectors with triggering efficiencies per detector in the range 0.005–0.02. Thus, typically total efficiencies $\Omega_T = N\Omega_\gamma$ were $\simeq 0.1$. Under these conditions it is not possible to infer M_γ with any certainty from the number of detectors k that fire in a given event. Fig. 1 exemplifies this by giving the probability $P_{Nk}(M_\gamma)$ that k out of $N = 20$ detectors fire, each with efficiency $\Omega_\gamma = 0.008$, when M_γ γ-rays are emitted. For this case $P_{Nk}(M_\gamma)$ is given by eq. (16) of ref. [3].

A completely different situation arises when $\Omega_T \equiv N\Omega_\gamma$ approaches unity. Ideally, for $N \gg M_\gamma$ with $\Omega_T \to 1$, the number of detectors k that fire in an event uniquely gives M_γ. Realistically, Ω_T can be made 0.95 ± 0.02 and $N \geqslant 2\, M_\gamma$ if shielding between individual detectors is not permitted. Such an instrument will provide M_γ from k with a rather small uncertainty.

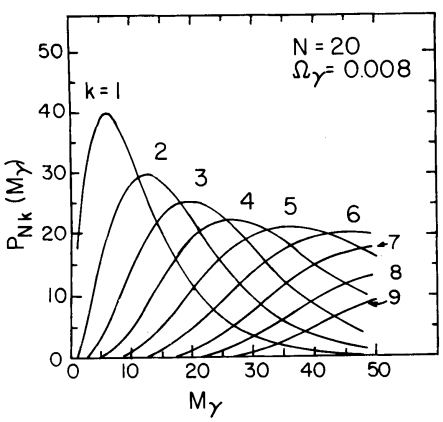

Fig. 1. Probability distributions $P_{Nk}(M_\gamma)$ for a k-fold coincidence as a function of γ-ray multiplicity, M_γ, for a system of twenty detectors each with an integral efficiency of 0.008. The distributions for $k = 1, 2, 3, 4, 5, 6, 7, 8$ and 9 are shown for M_γ up to 50.

Further considerations regarding the design of a "spin spectrometer" must include the possibility of recording the full energy and the related total γ-ray energy released with as high an efficiency as possible. Such information is essential in determining the population of the so-called "enrty states" defined as the states at (E^*, J) after particle emission. The requirement for a high efficiency for total energy detection is coupled indirectly to the choice of the number N of detectors and their size.

Other considerations regarding the design include the efficiency for observing a signal in several detectors when none of their immediate neighbors trigger. Such events give pulse heights equal to the transition energy E_γ of individual γ-rays with high probability. The number n of such occurrences out of k detectors that fire increases with the number of detectors N and may be a significant factor influencing the choice of N in a given instrument when energy correlations are considered.

The angular resolution in obtaining angular correlations and the time resolution for correlations in time are somewhat less important in determining the number of detectors N in the spectrometer.

In the following sections we shall give the theory for obtaining the response of the spectrometer for a given input of M_γ γ-rays with energies $\{E_i\}_{i=1,\ldots,M_\gamma}$.

2. Theory

2.1. General considerations

In the following discussion it will be understood that together with the spectrometer one or more additional selective detectors will be used in each experiment. In most cases the selective detectors will also be the gating detectors which define an "event" and require the response of the instrument to be noted. In certain cases some or all of the detectors in the spectrometer that respond may be used to define an event. A large variety of selective detectors should be compatible with the spectrometer. These could be classified as internal and as external to the spectrometer. Internal selective detectors should be placed in the hollow cavity of the spectrometer and could include one or more high resolution Ge(Li)

detectors, several ΔExE heavy-ion or light-particle identifying telescopes, small avalanche counters, mini-orange type e^- spectrometers, etc. External selective detectors should be placed outside the spectrometer and should view the target by removing individual NaI detector elements. These may include large NaI detectors, anti-Compton spectrometers, neutron time-of-flight detectors, large avalanche counters, etc.

2.2. Experimentally observable quantities

It is convenient to classify the reactions to be studied into two classes depending upon the number of reaction products that emit detectable γ-radiation. In the first class we include all reactions that produce only one residual nucleus that emits γ-rays. The most common process in this class is fusion, but for higher energies incomplete fusion, in which different parts of the projectile are captured by the target, may be considered. In all these cases particle emission usually precedes γ-decay and each reaction residue is formed in an "entry state" at excitation energy E^* and spin J. This state then de-excites to the ground state via an observable γ-cascade.

For heavy-ion collisions resulting in more than one excited product that emits γ-rays, the observed γ-cascade will be the sum of two or more cascades that de-excite the reaction products. In this class of processes we include quasi-elastic scattering, deeply inelastic scattering, Coulomb excitation with both projectile and target excited, prompt fission, sequential fission, etc.

Consider now a selective detector that singles out a particular class of events α at a rate $Q_s^{(\alpha)}$ given by $Q_s^{(\alpha)} = \sigma_\alpha \Omega_g^{(\alpha)}$, where σ_α is the cross section for the process of interest and $\Omega_g^{(\alpha)}$ is the efficiency of the selective detector including the solid angle. The γ-cascades to be investigated with the spectrometer dissipate a total excitation energy E^* and angular momentum ΔJ in a cascade of M_γ γ-rays with an energy spectrum $\{E_i\}_{i=1,\ldots,M_\gamma}$. For the first class of mechanisms the total energy E^* coincides with the entry state excitation and ΔJ is the difference between the entry and ground state angular momenta. For the second class of mechanisms the total energy and angular momentum dissipated are given by the sum of two or more entries to ground state cascades.

Consider now the first class of processes. The de-excitation of an entry state (E^*, J) to $(0, J_{gs})$ can in principle procede via a rather large number of pathways giving rise to many possible γ-cascades. A large number of observations of the decay $(E^*, J) \rightarrow (0, J_{gs})$ will result in a spectrum $n(E)\,\mathrm{d}E = \Sigma_i\, n(E_i)\,\mathrm{d}E_i$ where $n(E_i)$ is the number of transitions with energy between E_i and $E_i + \mathrm{d}E_i$ for the path i. The integral of such a spectrum gives the average $\langle M_\gamma \rangle$. Thus, there is an average cascade that can represent the de-excitation of a given entry state to the ground state. When referring to the multiplicity of a γ-cascade de-exciting an entry state we shall use the same symbol M_γ for the above average. Now the set of N detectors of the spectrometer (each with detection efficiency $\Omega_{\gamma,i}$) is examined in coincidence with the selective detector and the outcome of the measurement is a collection of pulse heights $\{h_j\}_{j=1,\ldots,k}$ in response to $M_\gamma^{(i)}$ γ-rays emitted in the reaction.

The maximum information is contained in the probability $P_{Nk,h_1,\ldots,h_N}(M_\gamma)$ that detector 1 records pulse height h_1, etc., when only k of $h_1,\ldots,h_N$ are above threshold. These probabilities can be extracted experimentally from the associated coincidence rates

$$Q^{(\alpha)}_{c,k,h_1,\ldots,h_N} = \sigma_\alpha \Omega_g^{(\alpha)} P^{(\alpha)}_{Nk,h_1,\ldots,h_N}(M_\gamma) \qquad (1)$$

as the ratios $Q^{(\alpha)}_{c,k,h_1,\ldots,h_N}/Q_s^{(\alpha)}$. More limited information can be extracted if one reports only the probabilities $P^{(\alpha)}_{NkH(M_\gamma)}$ associated with coincidence events when k out of N detectors fire above a threshold h_{th} and the total pulse height is

$$H \equiv \sum_{l=1}^{k} h_l \,.$$

Even more limited information is obtained by reporting the probabilities $P^{(\alpha)}_{N,k}(M_\gamma)$ that k out of N detectors fire above a threshold h_{th}.

It is quite clear that the angular correlation information for the $\{E_j\}_{j=1,\ldots,M_\gamma}$ cascade is contained in $P_{Nk,h_1,\ldots,h_N}(M_\gamma)$ despite the complications arising from the possibility that a given detector may have recorded either two or more γ-rays of a γ-ray scattered from another detector in the apparatus.

The detection probabilities can be classified according to the time evolution by giving the probability $P_{Nk,h_1t_1\Delta t_1,\ldots,h_Nt_N\Delta T_N}(M_\gamma)$ for detector 1 recording pulse height h_i in a time interval between t_1 and $t_1 + \Delta t_1$, etc. Most often, however, we may be interested in reporting $P_{Nk,mt}(M_\gamma)$ giving the probability that k out of N detectors are in prompt coincidence with the gating detector and m in delayed

coincidence occurring between t and $t + \Delta t$.

We shall be interested in predicting the response of the spectrometer to the above mentioned experimental situations.

2.3. The response of the instrument

2.3.1. Detection statistics and generating functions

There are several physical effects that contribute to the detection statistics and thus determine the performance of the spectrometer. These are: (a) *Incomplete detection* that arises from the fact that for a realistic nearly 4π instrument the total detection efficiency Ω_T is less than 1. This reduced efficiency leads to finite probabilities for different numbers of γ-rays escaping detection when M_γ are emitted in a given event. (b) *Crystal-to-crystal scattering* that arises from lack of shielding between detector elements. The lack of shielding is necessary to counteract the effect of (a) above. A consequence of this is the fact that one or more detector elements may respond to a single γ-ray. (c) *Coincidence summing* that arises from the finite probability that more than one γ-ray from a given event may strike the same detector element simultaneously causing a single response. (d) *Indistinguishable pulses* arising from the fact that in addition to γ-rays detection of particles such as neutrons or high energy protons etc., is possible in a given detector element. A small probability exists that such indistinguishable pulses may accompany a given nuclear event, despite the fact that the apparatus may be designed to distinguish pulses from most of the associated particles which can trigger one or more detector elements. Indistinguishable pulses may in turn cause responses of the type (a) through (c) described above.

The general formalism for the detection statistics can be derived by giving the complete response of the instrument to a single incident γ-ray or particle accounting for all the possibilities described in (a) through (d) above. This is accomplished by constructing the generating function in terms of the appropriate counting variables. We shall postpone the discussion of time dependence of the detection probabilities and shall only consider simultaneous events. We introduce here the counting variables $(t_1,...,t_N)$ for observing the pulse heights $(h_1,...,h_N)$ and the counting variables $(s_1,...,s_N)$ for enumerating the number of γ-rays striking a given detector. The generating function for the outcome due to a single incident γ-ray of energy E_γ is

$$
\begin{aligned}
G_1^{(\gamma)}(t_1,...,t_N;s_1,...,s_N) &= 1 - \sum_{i=1}^{N}\sum_{\kappa}\Omega_i^{(\gamma)}(h_\kappa) \\
&- \sum_{\substack{ij=1\\ i\neq j}}^{N}\sum_{\kappa\lambda} T_{ij}^{(\gamma)}(h_\kappa h_\lambda) \\
&+ \sum_{i=1}^{N}\sum_{\kappa}^{E_\gamma}\Omega_i^{(\gamma)}(h_\kappa)\, t_i^{h_\kappa} s_i \\
&+ \sum_{\substack{ij=1\\ i\neq j}}^{N}\sum_{\kappa\lambda} T_{ij}^{(\gamma)}(h_\kappa h_\lambda)\, t_i^{h_\kappa} t_j^{h_\lambda} s_i s_j\,, \qquad (2)
\end{aligned}
$$

where $\Omega_i^{(\gamma)}(h_\kappa)$ is the probability (efficiency) that for a γ-ray of energy E_γ only the ith detector records a pulse height h_κ, and $T_{ij}^{(\gamma)}(h_\kappa h_\lambda)$ is the probability that only the detectors i and j record pulse heights h_κ and h_λ, respectively. Inclusion of triple and higher order scattering terms, e.g., $T_{ijk}(h_\kappa h_\lambda h_\mu)$ for detectors ijk to record pulse heights h_κ, h_λ, h_μ, respectively, is straight forward. The latter become of importance when pair production becomes significant and single and double escape peaks are observed. The first three terms in eq. (2) correspond to no response, the fourth corresponds to the response of only one detector, and the last term to the response of any pair of detectors.

Ignoring the γ-ray angular correlation effects and considering a cascade $\{E_i\}_{i=1,...,M_\gamma}$ of M_γ statistically independent γ-rays we can write the generating function for $M_\gamma\gamma$-rays as

$$
\begin{aligned}
G_{M_\gamma}(t_1,...,t_N;s_1,...,s_N) &= \prod_{i=1}^{M_\gamma} G_1^{(i)}(t_1,...,t_N;s_1,...,s_N) \\
&= \sum_{\substack{h_1,...,h_N\\ n_1,...,n_N}} P(h_1,...,h_N;n_1,...,n_N) \\
&\times t_1^{h_1} t_2^{h_2},...,t_N^{h_N} s_1^{n_1} s_2^{n_2}...s_N^{n_N}\,, \qquad (3)
\end{aligned}
$$

where $P(h_1,...,h_N;\ n_1,...,n_N)$ is the probability for detector i to record h_i from n_i γ-rays that interacted with it, $i = 1,...,N$. $P(h_1,...,h_N;\ n_1,...,n_N)$, the coefficient of $t_1^{h_1} t_2^{h_2}...t_N^{h_N} s_1^{n_1} s_2^{n_2}...s_N^{n_N}$ in $G_{M_\gamma}(t_1,...,t_N;\ s_1,...,s_N)$, represents the maximal description of the response to

$$\{E_i\}_{i=1,...,M_\gamma} \rightarrow \{h_i\}_{i=1,...,k}\,.$$

2.3.2. Projections

More limited but very useful information can be

extracted more conveniently from the measurement $\{E_i\}_{i=1,\ldots,M_\gamma} \rightarrow \{h_i\}_{i=1,\ldots,k}$ in the following way. In the context of section 2.2 it may be possible to associate with the decay $(E, J) \rightarrow (0, J_{gs})$ an "average" or representative cascade $\{E_j\}_{j=1,\ldots,M_\gamma}$ corresponding to (E, M_γ). In this case the input to the apparatus is (E, M_γ) with $\{E_j\}_{j=1,\ldots,M_\gamma}$ such that

$$E = \sum_{j=1}^{M_\gamma} E_j$$

and the instrument will respond with a total pulse height

$$H = \sum_{i=1}^{k} h_i$$

where the sum is over the k out of N detectors that recorded pulse heights $h_i > h_{th}$. The probability distribution $P_{NHk}(E, M_\gamma)$ for this outcome must now be derived. Ignoring for the moment "$s_1,\ldots,s_N$" in the generating function we find that the probability P_{NH} is

$$P_{NH} = \sum_{h_1,\ldots,h_N} P_{h_1,\ldots,h_N} \delta^H_{h_1+\ldots+h_N} , \tag{4}$$

where $P_{h_1,\ldots,h_N}$ is the probability for a response $h_1,\ldots,h_N$. Then

$$\begin{aligned} \sum_{H=0}^{\infty} P_{NH} t^H &= \sum_{h_1,\ldots,h_N} P_{h_1,\ldots,h_N} t^{h_1+\ldots+h_N} \\ &= \sum_{h_1,\ldots,h_N} P_{h_1,\ldots,h_N} t_1^{h_1} \ldots t_N^{h_N} \Big|_{t_1=t_2=\ldots=t_N=t} \\ &= G_{M_\gamma}(t, t, \ldots, t) , \end{aligned} \tag{5}$$

so P_{NH} is the coefficient of t^H in $G_{M_\gamma}(t,\ldots,t)$. Restoring $s_1 \ldots s_N$, eq. (5) becomes

$$\begin{aligned} &G(s_1 \ldots s_N, t \ldots t) \\ &= \sum_{n_1 \ldots n_N} \sum_{H=0}^{\infty} P_{NH}(n_1 \ldots n_N)\, s_1^{n_1} \ldots s_N^{n_N} t^H . \end{aligned} \tag{6}$$

Here $P_{NH}(n_1 \ldots n_N)$ represents the probability that detector i responds to n_i γ-rays, $i = 1 \ldots N$ when the spectrometer gives a total pulse height H. The probability that precisely k detectors fire with $h_i > h_{th}$ is

$$P_{NHk}(E, M_\gamma) = \sum_{n_1 \ldots n_N} P_{NH}(n_1 \ldots n_N)\, \delta^{N-k}_{\delta^0_{n(1)}+\ldots+\delta^0_{n(N)}}$$

[where the sub-subscripts $n(1)$ and $n(N)$ denote the sub-subscripts n_1 and n_N respectively] so that the generator for $P_{NHk}(E, M_\gamma)$ is

$$\begin{aligned} F(t, s) &= \sum_{H,k=0}^{\infty} P_{NHk} t^H s^k \\ &= \sum_{H=0}^{\infty} t^H \sum_{n_1 \ldots n_N} P_{NH}(n_1 \ldots n_N)\, s^{N-\delta^0_{n(1)}-\ldots-\delta^0_{n(N)}} . \end{aligned} \tag{7}$$

The latter relation reduces to (see Appendix A)

$$\begin{aligned} F(t, s) &= \sum_{n=0}^{N} s^N (1-s)^{N-n} \\ &\times \sum_{\substack{0 \leqslant i_1,\ldots,i_N \leqslant 1 \\ i_1+\ldots+i_N=n}}{}' G_{M_\gamma}(t,\ldots,t; i_1,\ldots,i_N) , \end{aligned} \tag{8}$$

where the constrained sum can be averaged over all detector labellings of n detector responses to give

$$F(t, s) = \sum_{n=0}^{\infty} s^n (1-s)^{N-n} \binom{N}{n} G(t, n) . \tag{9}$$

We note that $F(t, s)$ is also the generator of the product moments for the bivariate distribution $P_{NHk}(E, M_\gamma)$ of the variables H and k. Interestingly, by setting $t = 1$ we are suppressing all pulse height information and $F(1, s)$ is the generator for $P_{Nk}(E, M_\gamma)$. Setting $t = 1$ in eq. (9) gives for the coefficient of s^k

$$P_{Nk}(E, M_\gamma) = (-1)^k \binom{N}{k} \sum_{n=0}^{k} (-1)^n \binom{k}{n} G(1, n) , \tag{10}$$

as found earlier [3].

The generating function $F(1, s)$ can be obtained either from the constrained sum of eq. (8) using (2) and (3) or from eqs. (2) and (3) in the following symmetrized model. If we wish to describe the response of the instrument only in terms of a few efficiency parameters we can average out the twofold and threefold correlations, recognizing that in so doing we alter somewhat the effect of the response correlations and therefore to some extent the result $P_{Nk}(E, M_\gamma)$. However, the symmetrized model should be a reasonable approximation if the response of the instrument is to be given in terms of the total efficiencies for only single triggering Ω' and double triggering Ω'' as defined by

$$\begin{aligned} \Omega' &\equiv \sum_{i=1}^{N} \sum_{\kappa} \Omega_i^{(\gamma)}(h_\kappa) = N \sum_{\kappa} \Omega^{(\gamma)}(h_\kappa) \\ &= N \Omega_\gamma (1 - F_\gamma) = \Omega_T (1 - F_\gamma) , \end{aligned} \tag{11}$$

$$\Omega'' \equiv \sum_{ij}\sum_{\kappa\lambda} T_{ij}(\gamma)(h_\kappa h_\lambda) = N(N-1)\sum_{\kappa\lambda} T^{(\gamma)}(h_\kappa h_\lambda)$$
$$= N(N-1)\langle T\rangle = N\Omega_\gamma E_\gamma = \Omega_T F_\gamma\,, \qquad (12)$$

with

$$F_\gamma \equiv \frac{\Omega''}{\Omega' + \Omega''} = \frac{\Omega''}{\Omega_T} = \frac{N(N-1)\langle T\rangle}{N\Omega_\gamma}\,, \qquad (13)$$

where, for an incident γ-ray of energy E_γ, $\Omega^{(\gamma)}(h_\kappa)$ gives the probability of recording a pulse height h_κ in any one of the N equivalent detectors in the spectrometer when no other detector responds, the summations over κ and λ are over pulse height from h_{th} to E_γ, Ω_γ gives the probability per detector element for triggering above threshold irrespective of whether the other elements respond or not, Ω_T gives the total probability (for N detectors) for triggering above threshold, $T^{(\gamma)}(h_\kappa h_\lambda)$ gives the probability for a double response with pulse height h_κ and h_λ, $\langle T\rangle$ gives the average triggering probability for double response above the discriminator and F_γ is the fraction for double triggers.

Experimentally Ω' is determined from the rate of 1-fold events per detector element in the spectrometer by multiplying it by the number of detectors present. Similarly F_γ is determined from the rate of $(N-1)$ 2-fold events coincident with a given detector element by dividing it by the singles rate (1-fold plus 2-fold events) in that given detector, using monoenergetic standard sources. In the following we assume that Ω', Ω'' and F_γ are independent of the number of detector elements N. In contrast, the singles efficiency Ω_γ varies as $1/N$, since $\Omega_\gamma = \Omega_T/N$. These considerations are important when different instruments of this type are to be compared. In the symmetrized model

$$G(t,n) = \prod_{\gamma=1}^{M_\gamma}\Big(1 - N\sum_\kappa \Omega_\kappa^{(\gamma)}(h_\kappa) - N(N-1)\sum_{\kappa\lambda} T^{(\gamma)}(h_\kappa h_\lambda) + n\sum_\kappa \Omega_\kappa^{(\gamma)}(h_\kappa)\, t^{h_\kappa} + n(n-1)\sum_{\kappa\lambda} T^{(\gamma)}(h_\kappa h_\lambda)\, t^{h_\kappa + h_\lambda}\Big)\,, \qquad (14)$$

where $T^{(\gamma)}(h_\kappa h_\lambda)$ is the average probability for a pair of detectors to record pulse heights h_κ and h_λ. In terms of Ω' and Ω'' or in terms of Ω_γ and F_γ we obtain

$$G(1,n) = \prod_{\gamma=1}^{M_\gamma} K_\gamma(n)$$

with

$$K_\gamma(n) = 1 - \Omega'\left(1 - \frac{n}{N}\right) - \Omega''\left(1 - \frac{n(n-1)}{N(N-1)}\right)$$
$$= 1 - N\Omega_\gamma\left\{1 - \frac{n}{N}\left[1 - F_\gamma\left(1 - \frac{n-1}{N-1}\right)\right]\right\}. \qquad (16)$$

In the symmetrized model the effect of detecting other particles such as neutrons is easily incorporated. For x incident neutrons with an efficiency of detection Ω_ν and scattering F_ν we obtain

$$K_\nu(n) = 1 - N\Omega_\nu\left\{1 - \frac{n}{N}\left[1 - F_\nu\left(1 - \frac{n-1}{N-1}\right)\right]\right\} \qquad (17)$$

and $G(1,n)$ becomes

$$G(1,n) = G_\gamma(1,n)\, G_\nu(1,n) \qquad (17a)$$

where

$$G_\gamma(1,n) = \prod_{\gamma=1}^{M_\gamma} K_\gamma(n) \text{ and } G_\nu(1,n) = \prod_{\nu=1}^{x} K_\nu(n)\,.$$

A further approximation leads to simpler expressions. If all $M_\gamma\gamma$-rays and x neutrons are assumed to have the same average efficiencies $\bar{\Omega}_\gamma$ and $\bar{\Omega}_\nu$ then we can write

$$\bar{G}(1,n) = \bar{K}_\gamma(n)^{M_\gamma}\bar{K}_\nu(n)^x\,, \qquad (17b)$$

where $\bar{K}_\gamma(n)$ and $\bar{K}_\nu(n)$ are evaluated with $\bar{\Omega}_\gamma$ and $\bar{\Omega}_\nu$. This approximation is useful in evaluating the expected performance of the instrument but it should

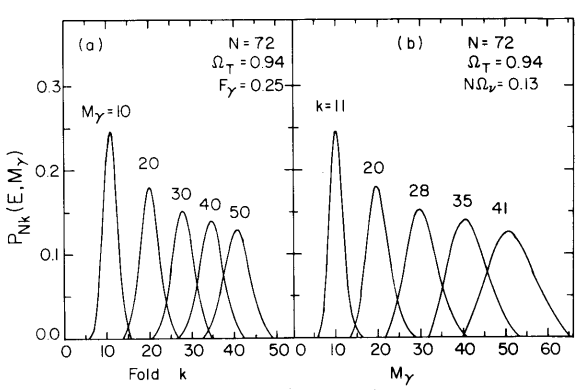

Fig. 2. In part (a) the distributions in fold k are given for 72 detectors, a total γ-ray detection efficiency $\Omega_T = 0.94$, a scattering fraction $F_\gamma = 0.25$ and a total neutron detection efficiency $N\Omega_\nu = 0.13$. Distributions for $M_\gamma = 10, 20, 30, 40$ and 50 are shown for compairsons. In part (b) the muliplicity distributions $P_{Nk}(M_\gamma)$ are shown for fixed $k = 11, 20, 28, 35$ and 41 which correspond to $\langle M_\gamma\rangle \simeq 10, 20, 30, 40$ and 50, respectively.

be avoided in analyzing experimental data.

Equations (17a) and (17b) are of fundamental importance in that in conjunction with eq. (10) they completely determine the response of the spectrometer to cascades of given multiplicity.

As an example of the properties of $P_{Nk}(E, M_\gamma)$ obtained from eqs. (10) and (17b) we show in fig. 2 a set of distributions evaluated for $N = 72$, $\Omega_T = 0.94$, $F_b = 0.25$ and $N\Omega_\nu = 0.13$. In fig. 2a the response distributions $P_{Nk}(E, M_\gamma)$ are given as a function of k for $M_\gamma = 10$, 20, 30, 40 and 50. In fig. 2b the response distributions $P_{Nk}(E, M_\gamma)$ are given as a function of M_γ for constant $k = 11$, 20, 28, 35 and 41. For the fold distributions (fig. 2a)

$$\sum_k P_{Nk}(E_\gamma, M_\gamma) = 1 ,$$

but for the multiplicity distributions (fig. 2b)

$$\sum_{M_\gamma} P_{Nk}(E, M_\gamma) \neq 1 .$$

It is seen that the fold distributions can be approximated well by Gaussian curves.

The bivariate distribution $P_{NHk}(E, M_\gamma)$ can in general be obtained as the coefficient of $t^H s^k$ in $F(t, s)$ of eq. (9), where k is the number of detectors responding with $\{h_1, ..., h_N\}$ and it is given by

$$P_{NHk}(E, M_\gamma) = \left(\frac{1}{2\pi i}\right)^2 \oint \frac{dt}{t^{H+1}} \oint \frac{ds}{s^{k+1}} F(t, s) . \qquad (18)$$

In the symmetrized model the integration over s can be carried out giving

$$P_{NHk}(E, M_\gamma) = (-1)^k \binom{N}{k} \sum_{n=0}^{k} (-1)^n \binom{k}{n} \mathcal{H}(H, n) \qquad (18a)$$

where

$$\mathcal{H}(H, n) = \left(\frac{1}{2\pi i}\right) \oint \frac{dt}{t^{H+1}} G(t, n) . \qquad (18b)$$

The complex structure of eq. (14) makes the analytic evaluation of eq. (18b) impractical. Considerable insight into the structure of $P_{NHk}(E, M_\gamma)$ can be obtained by introducing a very simple model. Consider M_γ incident γ-rays each with an average detection efficiency Ω_{E_γ} for the entire spectrometer. Ignoring the division into N detectors, we require that each of k' γ-rays produce a given pulse height $h = E_\gamma$ with efficiency Ω_{E_γ} and nothing otherwise. Then

$$F(t, s) = (1 - \Omega_{E_\gamma} + \Omega_{E_\gamma} s t^h)^{M_\gamma} \qquad (19)$$

for which eq. (18) is non-zero only for $H = k'h$ and

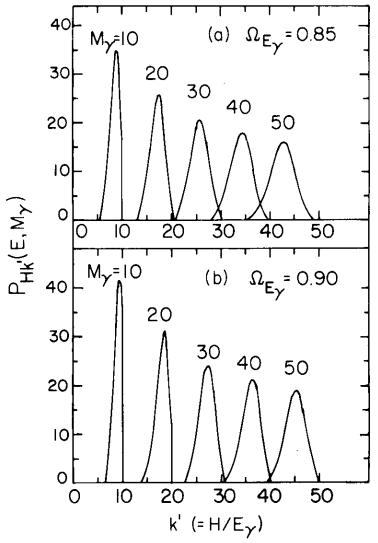

Fig. 3. Approximate total pulse height distributions $P_{Nk'}(E, M_\gamma)$ evaluated for an average detection efficiency $\Omega_T = 0.85$ and 0.90 for the entire spectrometer for different values of M_γ = 10, 20, 30, 40 and 50. The distributions are plotted versus k' which gives the total pulse-height in units of E_γ, the incident energy.

$P_{Hk'}(E, M_\gamma)$ is given by the binomial distribution function,

$$P_{Hk'}(E, M_\gamma) = \binom{M_\gamma}{k'} (1 - \Omega_{E_\gamma})^{M_\gamma - k'} \Omega_{E_\gamma}^{k'} , \qquad (20)$$

where the total pulse height is $H = k'h = k'E_\gamma$, and it is given by k' in units of E_γ. Clearly, k' differs from k, which is the number of detectors that fire when N are present in the spectrometer. For realistic values of $\Omega_{E_\gamma} \sim 0.60$–$0.90$ eq. (20) gives distributions in H which could adequately be described in terms of their first few moments. Some of the binomial distributions of eq. (20) are plotted in fig. 3 for $\Omega_{E_\gamma} = 0.85$ and 0.90 as a function of k' for $M_\gamma = 10$, 20, 30, 40 and 50. It is seen that these curves have a small tail toward the low k' side, corresponding to a small negative skewness.

2.3.3. Moment expansions for $P_{NHk}(E, M_\gamma)$

The various moments of $P_{NHk}(E, M_\gamma)$ with respect to k and H can be easily derived from eq. (9), since

$$F(1, 1) = 1 ,$$

$$\frac{\partial}{\partial s} F(t, s)\Big|_{t=s=1} = \langle k \rangle ,$$

$$\left.\frac{\partial^2}{\partial s^2} F(t, s)\right|_{t=s=1} = \langle k(k-1)\rangle \text{ , etc.,}$$

and

$$\left.\frac{\partial}{\partial t} F(t, s)\right|_{t=s=1} = \langle H\rangle \text{ ,}$$

$$\left.\frac{\partial^2}{\partial t^2} F(t, s)\right|_{t=s=1} = \langle H(H-1)\rangle \text{ , etc.}$$

In general,

$$\left.\frac{\partial^m}{\partial t^m}\frac{\partial^p}{\partial s^p} F(t, s)\right|_{t=s=1} = \langle k(k-1)\ldots(k-p+1) \times H(H-1)\ldots(H-m+1)\rangle \text{ .} \quad (21)$$

More specifically, these product moments k_n are given by

$$k_1 \equiv \langle k\rangle = N[1 - G(1, N-1)] \text{ ,} \quad (22a)$$

$$k_2 \equiv \langle k(k-1)\rangle = N(N-1)[1 - 2G(1, N-1) + G(1, N-2)] \text{ , etc.,} \quad (22b)$$

and

$$k_n \equiv \langle k(k-1)\ldots(k-n+1)\rangle = \frac{N!}{(N-n)!}\sum_{l=0}^{n}\binom{n}{l} \times (-1)^l G(1, N-l) \text{ .} \quad (22c)$$

Using eqs. (17a) or (17b) we derive, respectively:

$$G(1, N-l) = \prod_{\gamma=1}^{M_\gamma}\left[1 - l\Omega_\gamma\left(1 + F_\gamma\frac{N-l}{N-1}\right)\right] \times \prod_{\nu=1}^{x}\left[1 - l\Omega_\nu\left(1 + F_\nu\frac{N-l}{N-1}\right)\right]$$

or

$$G(1, N-l) = \left[1 - l\bar{\Omega}_\gamma\left(1 + \bar{F}_\gamma\frac{N-l}{N-1}\right)\right]^{M_\gamma} \times \left[1 - l\bar{\Omega}_\nu\left(1 + \bar{F}_\nu\frac{N-l}{N-1}\right)\right]^{x} \text{ .} \quad (22e)$$

The first few moments about the origin $\rho_n \equiv \langle k^n\rangle$ can be obtained from the product moments k_n via

$$\rho_0 = k_0 = 1 \text{ ,} \quad (23)$$

$$\rho_1 = \langle k\rangle = k_1 \text{ ,} \quad (23a)$$

$$\rho_2 = \langle k^2\rangle = k_2 + k_1 \text{ ,} \quad (23b)$$

$$\rho_3 = \langle k^3\rangle = k_3 + 3k_2 + k_1 \text{ ,} \quad (23c)$$

$$\rho_4 = \langle k^4\rangle = k_4 + 6k_3 + 7k_2 + k_1 \text{ .} \quad (23d)$$

The central moments defined as the moments about the mean are related to those about the origin via

$$\mu_n = \sum_{j=0}^{n}\binom{n}{j}(-1)^{n-j}\rho_j\rho_1^{n-j} \text{ ,} \quad (24)$$

with

$$\mu_0 = \rho_0 = 1, \mu_1 = 0 \text{ ,} \quad (24a)$$

$$\mu_2 \equiv \sigma_k^2 = \rho_2 - \rho_1^2 = k_2 + k_1 - k_1^2 \text{ ,} \quad (24b)$$

$$\mu_3 = \rho_3 - 3\rho_2\rho_1 + 2\rho_1^3 = k_3 - 3k_2(k_1 - 1) + k_1(k_1 - 1)(2k_1 - 1) \text{ , etc.} \quad (24c)$$

The skewness s_k and excess e_k are defined by

$$s_k \equiv \frac{\mu_3}{\mu_2^{3/2}} \text{ and } e_k \equiv (\mu_4/\mu_2^2) - 3 \text{ .} \quad (24d)$$

Using average efficiencies we find for $\langle k\rangle$ that

$$\langle k\rangle = N\{1 - [1 - \bar{\Omega}_\gamma(1 + \bar{F}_\gamma)]^{M_\gamma}[1 - \bar{\Omega}_\nu(1 + \bar{F}_\nu)]^{x}\} \text{ ,} \quad (25)$$

which can be solved for M_γ to give

$$M_\gamma = \frac{\ln(1 - \langle k\rangle/N) - x\ln[1 - \bar{\Omega}_\nu(1 + \bar{F}_\nu)]}{\ln[1 - \bar{\Omega}_\gamma(1 + \bar{F}_\gamma)]} \text{ .} \quad (25a)$$

More elaborate, but explicit expressions for the higher moments σ_k, s_k and e_k can be obtained using eqs. (24b) through (24d).

We derive next the first few moments of $P_{NHk}(E, M_\gamma)$ with respect to H, the total pulse height. Eq. (21) gives

$$H_1 \equiv \langle H\rangle = \left.\frac{\partial F(t, s)}{\partial t}\right|_{s,t=1} = \left.\frac{\mathrm{d}}{\mathrm{d}t}G_\gamma(t, N) + \frac{\mathrm{d}}{\mathrm{d}t}G_\nu(t, N)\right|_{t=1} \text{ .} \quad (26)$$

Let us define the spectral function $\omega_l^{(\alpha)}$ for $l \geqslant 1$ as

$$\omega_l^{(\alpha)} \equiv N\sum_\kappa \Omega^{(\alpha)}(h_\kappa)\, h_\kappa^l + N(N-1) \times \sum_{\kappa\lambda} T^{(\alpha)}(h_\kappa h_\lambda)(h_\kappa + h_\lambda)^l + \ldots \text{ ,} \quad (27)$$

where α is a label for γ-rays or neutrons etc. Using eq. (14) in expression (26) we obtain

$$\langle H\rangle = \sum_{\gamma=1}^{M_\gamma}\omega_1^{(\gamma)} + \sum_{\nu=1}^{x}\omega_1^{(\nu)} = \langle H_\gamma\rangle + \langle H_\nu\rangle \text{ .} \quad (28)$$

For the second moment with respect to H we find

from eq. (21)

$$H_2 \equiv \langle H(H-1)\rangle = \frac{d^2}{dt^2} G_\gamma(t, N) + 2 \frac{d}{dt} G_\gamma(t, N)$$

$$\frac{d}{dt} G_\nu(t, N) + \frac{d^2}{dt^2} G_\nu(t, N)\Big|_{t=1} . \quad (29)$$

Noting that $\sigma_H^2 = \langle H^2\rangle - \langle H\rangle^2 = H_2 + H_1 - H_1^2$ we find

$$\sigma_H^2 = \sigma_{H_\gamma}^2 + \sigma_{H_\nu}^2 , \quad (30)$$

where

$$\sigma_{H_\alpha}^2 = \frac{d^2}{dt^2} G_\alpha(t, N) + \frac{d}{dt} G_\alpha(t, N) - \left(\frac{d}{dt} G_\alpha(t, N)\right)^2\Big|_{t=1} . \quad (31)$$

Using eq. (14) after some algebra we find

$$\mu_{2H_\gamma} = \sigma_{H_\gamma}^2 = \sum_{\gamma=1}^{M_\gamma} (\omega_2^{\{\gamma\}} - \omega_1^{\{\gamma\}2}) \quad (32)$$

and

$$\mu_{2H_\nu} = \sigma_{H_\nu}^2 = x(\omega_2^{\{\nu\}} - \omega_1^{\{\nu\}2}) , \quad (32a)$$

where the neutrons were treated with average efficiencies for given neutron multiplicity x.

From the third product moment in $H_3 \equiv \langle H(H-1)(H-2)\rangle$ we find for the third central moment that

$$\mu_{3H} = H_3 - 3H_2(H_1 - 1) + H_1(H_1 - 1)(2H_1 - 1) . \quad (33)$$

Using eq. (21) we can show that

$$\mu_{3H} = \mu_{3H_\gamma} + \mu_{3H_\nu} , \quad (33a)$$

where

$$\mu_{3H_\alpha} = \frac{d^3}{dt^3} G_\alpha(t, N) - 3\frac{d^2}{dt^2} G_\alpha(t, N)\left(\frac{d}{dt} G_\alpha(t, N) - 1\right) + \frac{d}{dt} G_\alpha(t, N)\left(\frac{d}{dt} G_\alpha(t, N) - 1\right)\left(2\frac{d}{dt} G_\alpha(t, N) - 1\right)\Big|_{t=1}$$

After considerable algebra we obtain

$$\mu_{3H_\gamma} = \sum_{\gamma=1}^{M_\gamma} (\omega_3^{\{\gamma\}} - 3\omega_2^{\{\gamma\}}\omega_1^{\{\gamma\}} + 2\omega_1^{\{\gamma\}3}) , \quad (33c)$$

with a similar expression for μ_{3H_ν}.

It is possible to generalize the moments and write for $n = 2,3$, $\mu_{nH} = \mu_{nH_\gamma} + \mu_{nH_\nu}$ where

$$\mu_{nH_\alpha} = \sum_{\gamma=1}^{M_\gamma} \left(\sum_{j=0}^{n} \binom{n}{j} (-1)^{n-j} \omega_j^{\{\alpha\}} \omega_1^{\{\alpha\}n-j}\right) \quad (34a)$$

or

$$\mu_{nH_\alpha} = M_\gamma \left(\sum_{j=0}^{n} \binom{n}{j} (-1)^{n-j} \omega_j^{\{\alpha\}} \omega_1^{\{\alpha\}n-j}\right) , \quad (34b)$$

where for the applicability of this formula we must set $\omega_0^{\{\alpha\}} = 1$. This is to be contrasted with the value of $\omega_0^{\{\alpha\}} = \Omega_T^{\{\alpha\}}$ from eqs. (27), (11) and (12).

Finally, we derive an expression for the correlation coefficient $\rho_{Hk} \equiv \langle Hk\rangle / \langle H\rangle\langle k\rangle$ between the variables H and k.

From eq. (21) we obtain

$$\langle Hk\rangle = N\langle H\rangle - N\frac{d}{dt} G(t, N-1)\Big|_{t=1} \quad (35)$$

with

$$\frac{d}{dt} G(t, N-1)\Big|_{t=1} = G_\nu(1, N-1)\frac{d}{dt} G_\gamma(t, N-1) + G_\gamma(1, N-1)\frac{d}{dt} G_\nu(t, N-1)\Big|_{t=1} . \quad (35a)$$

In the approximation of average multiplicities M_γ and x with average efficiencies $\bar{\Omega}_\gamma$ and $\bar{\Omega}_\nu$ for γ-rays and neutrons the above functions can be simplified as follows:

$$G_\gamma(1, N-1) = [1 - \bar{\Omega}_\gamma(1 + \bar{F}_\gamma)]^{M_\gamma} , \quad (36)$$

$$G_\nu(1, N-1) = [1 - \bar{\Omega}_\nu(1 + \bar{F}_\nu)]^{x} , \quad (36a)$$

$$\frac{d}{dt} G_\gamma(t, N-1)\Big|_{t=1} = \left(\frac{N-1}{N}\right)\left(\langle H_\gamma\rangle - M_\gamma N \times \sum_{\kappa\lambda} T^{(\gamma)}(h_\kappa h_\lambda)(h_\kappa + h_\lambda)\right) \times [1 - \bar{\Omega}_\gamma(1 + \bar{F}_\gamma)]^{M_\gamma - 1} \quad (36b)$$

$$\frac{d}{dt} G_\nu(t, N-1)\Big|_{t=1} = \left(\frac{N-1}{N}\right)\left(\langle H_\nu\rangle - xN \times \sum_{\kappa\lambda} T^{(\nu)}(h_\kappa h_\lambda)(h_\kappa + h_\lambda)\right) \times [1 - \bar{\Omega}_\nu(1 + \bar{F}_\nu)]^{x-1} . \quad (36c)$$

Since the term

$$M_\gamma N \sum_{\kappa\lambda} T^{(\gamma)}(h_\kappa h_\lambda)(h_\kappa + h_\lambda) .$$

is small compared with $\langle H_\gamma\rangle$ in eq. (36b) ($\sim 1/N$) and similarily in eq. (36c), a good lower limit for ρ_{Hk} is obtained by ignoring the sums compared to $\langle H_\gamma\rangle$ and $\langle H_\nu\rangle$. This gives

$$\rho_{Hk} \gtrsim \left[\frac{1}{U} - \frac{N-1}{N}\left(\frac{\langle H_\gamma\rangle/\langle H\rangle}{1-\bar{\Omega}_\gamma(1+\bar{F}_\gamma)} + \frac{\langle H_\nu\rangle/\langle H\rangle}{1-\bar{\Omega}_\nu(1+\bar{F}_\gamma)}\right)\right]\Big/\left(\frac{1}{U}-1\right) \quad (36d)$$

where $U = [1-\bar{\Omega}_\gamma(1+\bar{F}_\gamma)]^{M_\gamma}[1-\bar{\Omega}_\nu(1+\bar{F}_\nu)]^x$.

It should be mentioned here that ρ_{Hk} is important in the determination of the response of the instrument. For a given multiplicity M_γ it is clear that increasing the fold k results in an increase in H, so that H and k are positively correlated with ρ_{Hk} near unity. However, response to neutrons as indicated in eq. (36d) produces also a positive but different correlation between H and k.

3. Performance characteristics

3.1. Multiplicity resolution

As it was discussed in section 2.3.1 there are four factors that affect the performance of the spectrometer. These are: (1) incomplete detection; (2) crystal-to-crystal scattering; (3) coincidence summing; and (4) indistinguishable pulses, e.g., neutrons.

3.1.1. Incomplete detection and crystal-to-crystal scattering

It is possible to isolate the various effects described above in order to demonstrate their influence on the response to various cascades of known γ-multiplicity. For this purpose, in the limit $N\to\infty$, the coicidence summing is reduced to zero. In this case, eq. (10), that gives the response of the spectrometer, becomes difficult to evaluate numerically for large N. An expression for

$$\lim_{N\to\infty} P_{Nk}(E, M_\gamma)$$

can be obtained from eq. (9) written as

$$F(s) = \sum_{n=0}^{N} s^n(1-s)^{N-n}\binom{N}{n}\left[1-\frac{N-n}{N}\times\left(\Omega' + \Omega''\frac{N+n-1}{N-1}\right)\right]^{M_\gamma}. \quad (37a)$$

The result (see Appendix B) is:

$$\lim_{N\to\infty} P_{Nk}(E, M_\gamma) = M_\gamma! \sum_{n=0}^{k/2}\frac{(1-\Omega_T)^{M_\gamma+n-k}}{(M_\gamma+n-k)!}\times\frac{(\Omega'')^n}{n!}\frac{(\Omega')^{k-2n}}{(k-2n)!}. \quad (37b)$$

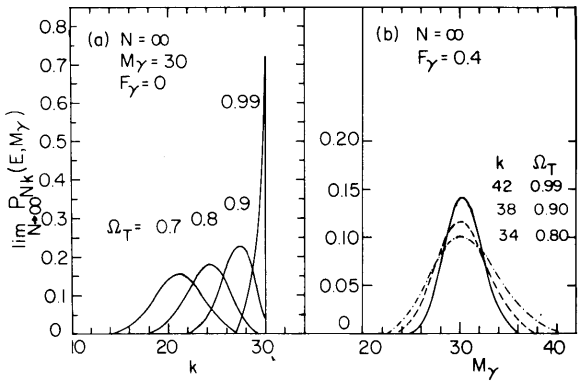

Fig. 4. In part (a) are shown plots of the $N\to\infty$ limit of the fold distributions evaluated for four values of the total detection efficiency $\Omega_T = 0.7, 0.8, 0.9$ and 0.99 for fixed $M_\gamma = 30$ and no scattering ($F_\gamma = 0$). In part (b) the multiplicity distributions are shown for the $N\to\infty$ limit for the indicated pairs of k and Ω_T values that give $\langle M_\gamma\rangle \simeq 30$. A fixed scattering fraction $F_\gamma = 0.4$ is used.

This equation in the limit $\Omega''\to 0$ and $\Omega_T\to 1$ gives a δ-function response versus k about $k = M_\gamma$.

In order to display the effect of incomplete detection on the resolution, we show in fig. 4a plots of

$$\lim_{N\to\infty} P_{Nk}(E, M_\gamma) \text{ versus } k$$

for four values of $\Omega_T = 0.99, 0.90, 0.80$ and 0.70 for fixed value of $M_\gamma = 30$ with no crystal-to-crystal scattering ($F_\gamma = 0$). The rapid loss of fold resolution $\Delta k/\langle k\rangle(\%)$ defined as the % full width at half maximum is clearly seen. Furthermore, it is seen that $\langle k\rangle$ decreases with decreasing Ω_T, and it can be shown to be given by $\langle k\rangle = M_\gamma\Omega_T(1+F_\gamma)$. In fig. 4b we show the effect of Ω_T to the response function by plotting

$$\lim_{N\to\infty} P_{Nk}(E, M_\gamma)$$

for pairs of values of k and Ω_T of 42 and 0.99 (solid curve), 38 and 0.90 (dashed curve) and 34 and 0.80 (dash–dot curve). These were evaluated for $F_\gamma = 0.4$ and correspond to $\langle M_\gamma\rangle \simeq 30$. It is seen that the multiplicity resolution $\Delta M_\gamma/\langle M_\gamma\rangle$ (%) decreases with decreasing Ω_T.

Realistic upper limits of the crystal-to-crystal scattering can be obtained from the peak-to-total ratios for NaI detectors of different sizes. An upper limit for F_γ is given by $(1-f_p)$ where f_p is the peak-to-peak total ratio. Fig. 5 shows calculated values [13] of $1-f_p$ for cylindrical NaI detectors with dimensions (diameter × length) of 7.6 cm × 7.6 cm (dashed curve), 12.7 cm × 10.2 cm (dash–dot curve),

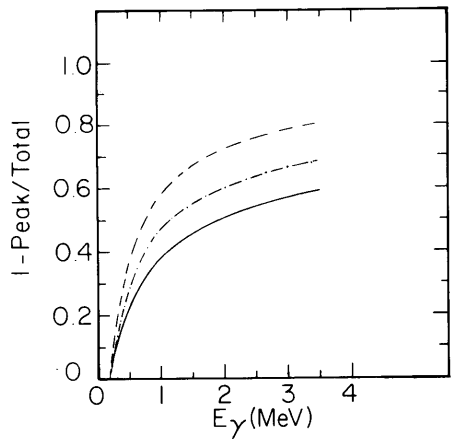

Fig. 5. Calculated values of the Compton-to-total ratio (1-peak/total) for cylindrical NaI detectors with dimensions diameter × length of 7.6 × 7.6 cm (dashed line), 12.7 × 10.2 cm (dash–dot line), and 12.7 cm × 17.8 cm (solid line) as a function of the incident γ-energy in MeV.

and 12.7 cm × 17.8 cm (solid curve). It is expected that a realistic spectrometer with large detector elements will have $F_\gamma \sim 0.2$–0.4 for typical energies of ~1 MeV.

In the limit of $N \to \infty$ the effect of incomplete detection on the resolution $\Delta M_\gamma/\langle M_\gamma\rangle$ is shown in fig. 6a as a function of Ω_T for $M = 30$ and for $F = 0$, 0.1, 0.2 and 0.4. Again the rapid loss in resolution with decreasing Ω_T is clearly seen.

The effect of crystal-to-crystal scattering on the multiplicity resolution is shown in fig. 6b, where the percent $\Delta M_\gamma/\langle M_\gamma\rangle$ is plotted versus F_γ for $N \to \infty$,

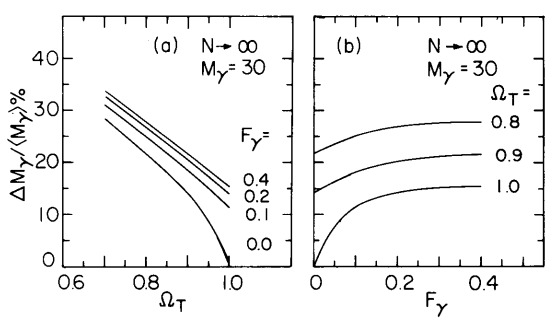

Fig. 6. Part (a) shows the dependence of the limiting ($N \to \infty$) percent multiplicity resolution ($\%\Delta M_\gamma/\langle M_\gamma\rangle$, ΔM_γ = fwhm) on the total detection efficiency Ω_T evaluated for four values of the scattering fraction $F_\gamma = 0.$ 0.1, 0.2 and 0.4 for fixed incident multiplicity $M_\gamma = 30$. Part (b) shows the dependence of the limiting ($N \to \infty$) multiplicity resolution on the scattering fraction F_γ for three values of Ω_T = 0.8, 0.9 and 1.0 evaluated for fixed γ-multiplicity $M_\gamma = 30$.

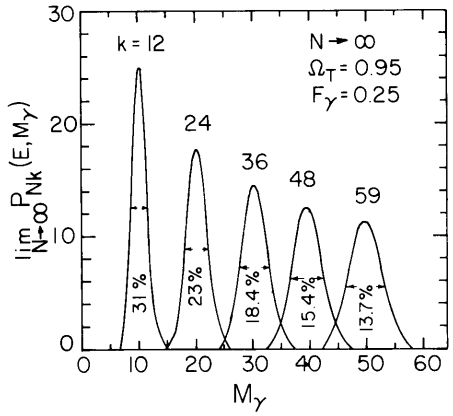

Fig. 7. Limiting response functions ($N \to \infty$) versus M_γ for k = 12, 24, 36, 48 and 59 corresponding to $\Omega_T = 0.95$ and a scattering fraction $F_\gamma = 0.25$. The percent $\Delta M_\gamma/\langle M_\gamma\rangle$ is given under each distribution.

$M_\gamma = 30$ and $\Omega_T = 1.0$, 0.9, and 0.80. It is seen that $\Delta M_\gamma/\langle M_\gamma\rangle$ increases at first rapidly with increasing F_γ and that it levels off for $F_\gamma \geqslant 0.15$.

In fig. 7 we show some response functions by plotting

$$\lim_{N\to\infty} P_{Nk}(E, M_\gamma)$$

versus M_γ for k = 12, 24, 36, 48 and 59 calculated with $\Omega_T = 0.95$, and $F_\gamma = 0.25$. This choice of folds gives responses with $\langle M_\gamma\rangle \simeq 10$, 20, 30, 40, and 50. The values of $\Delta M_\gamma/\langle M_\gamma\rangle$ are also given in % under each curve.

It is important to note that

$$\sum_{k=0}^{N} P_{Nk}(E, M_\gamma) = 1 \qquad \text{for } M_\gamma = \text{const.}, \tag{38}$$

whereas

$$\sum_{M_\gamma=0}^{\infty} P_{Nk}(E, M_\gamma) \neq 1 \qquad \text{for } k = \text{const.} \tag{38a}$$

3.1.2. Coincidence summing

The effect of coincidence summing is manifested because of the finite solid angle when a finite number of detectors is present. In this case eqs. (10) and (17b) can be used to evaluate the response functions. In order to demonstrate the main properties of the response functions it is sufficient to give $\langle k\rangle$ and $\Delta M_\gamma/\langle M_\gamma\rangle$. The values of $\langle k\rangle$ can very conveniently be calculated via eq. (25). The multiplicity resolution can be obtained via eqs. (23) and (25a). Since the

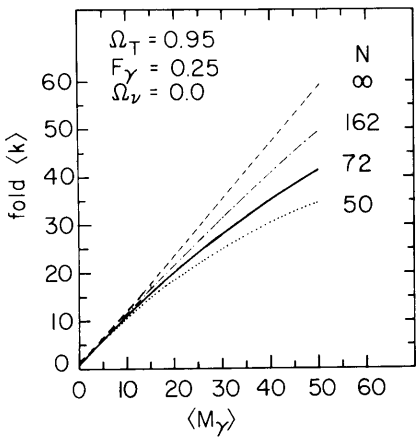

Fig. 8. Dependence of the average fold $\langle k \rangle$ on $\langle M_\gamma \rangle$ for spectrometers with N = 50, 72, 162 and ∞ evaluated for constant Ω_T = 0.95, F_γ = 0.25 and Ω_ν = 0. As the number of detectors decreases $\langle k \rangle$ tends to level off at high $\langle M_\gamma \rangle$.

fold distributions are nearly Gaussian in shape we obtain for the fwhm $\Delta k = 2.35\sigma_k$. Next we find $\langle M_\gamma \rangle \pm \frac{1}{2}\Delta M_\gamma$ from eq. (25a) using $\langle k \rangle \pm \frac{1}{2}\Delta k$ and thus obtain ΔM_γ by difference. The $\Delta M_\gamma / \langle M_\gamma \rangle$ values are larger than $\Delta k / \langle k \rangle$ for the same $\langle M_\gamma \rangle$, because the successive $\langle k \rangle$ values move closer as $\langle M_\gamma \rangle$ is increased. This is clearly demonstrated plotting $\langle k \rangle$ versus M_γ for various values of N. Such a plot is shown in fig. 8 for $\Omega_T = 0.95, F_\gamma = 0.25$ and $\Omega_T = 0$. As mentioned earlier for $N \to \infty$ and $M_\gamma \geqslant 1$ a linear dependence is obtained with a slope of $\Omega_T(1 + F)$. For finite N it is seen that $\langle k \rangle$ decreases progressively more with increasing M_γ as the number of detector elements N is decreased from 162 to 50.

The effect of finite N on the multiplicity resolution is demonstrated in fig. 9. The multiplicity resolution is plotted in fig. 9a as a function of Ω_T for different values of N keeping M_γ = 30 and F_γ = 0.25. The case $N \to \infty$ is also included for comparison. The loss of resolution with decreasing Ω_T is relatively more pronounced for systems with larger N. The effect of scattering is shown in fig. 9b for several values of N keeping M_γ = 30 and Ω_T = 0.96. It is seen that for $0.15 < F_\gamma < 0.4$ the resolution does not change significantly with F_γ. In order to illustrate the effect of the finite number of detectors on the multiplicity resolution as a function of M_γ we plot in fig. 10a the percent $\Delta M_\gamma / \langle M_\gamma \rangle$ versus N for fixed M_γ = 10, 20, 30, 40 and 50 keeping Ω_T = 0.95 and F_γ = 0.25. It is seen that the resolution improves considerably with increasing N for the high M_γ values. The horizontal arrows indicate the limiting resolution of each M_γ value in the $N \to \infty$ limit. In fig. 10b the percent $\Delta M_\gamma / \langle M_\gamma \rangle$ is plotted versus M_γ for $N = \infty$, 162, 92, 72 and 50. It is seen that for N = 50 $\Delta M_\gamma / \langle M_\gamma \rangle$ levels off and then increases for $M_\gamma \gtrsim 35$.

3.1.3. Detection of neutrons

Since the γ-detector elements may respond to neutrons, identification of neutron pulses by time-of-flight techniques is considered necessary. Due to flight path limitations complete characterization of

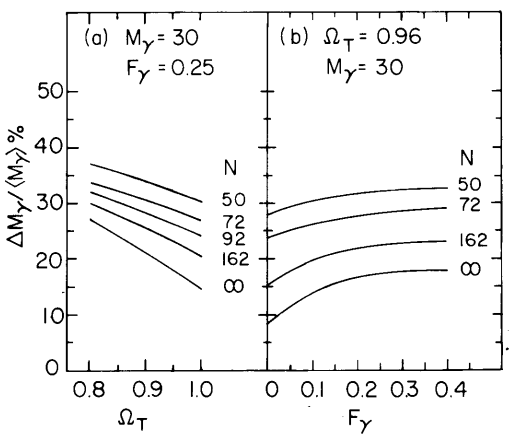

Fig. 9. Part (a) shows the dependence of the percent multiplicity resolution on total detection efficiency Ω_T for spectrometers with N = 50, 72, 92, 162 and ∞, evaluated for constant M_γ = 30 and F_γ = 0.25. Part (b) shows the dependence of the percent multplicity resolution on the scattering fraction F_γ for spectrometers with N = 50, 72, 162 and ∞ evaluated for fixed M_γ = 30 and Ω_T = 0.96.

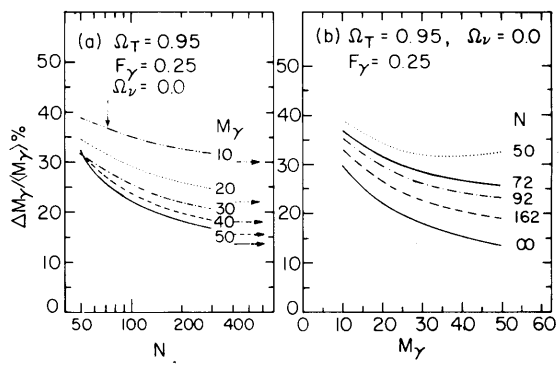

Fig. 10. Part (a) shows the dependence of the percent multiplicity resolution on the number of detector elements N for the indicated values of the multiplicity M_γ, evaluated with constant Ω_T = 0.95, F_γ = 0.25 and Ω_ν = 0. The horizontal arrows indicated the limiting resolutions for $N \to \infty$. Part (b) shows the variation of the multiplicity resolution with M_γ for spectrometers with N = 50, 72, 92, 162 and ∞, evaluated with constant Ω_T = 0.95, F_γ = 0.25 and Ω_ν = 0.

all the pulses may not be possible. Under these conditions some undersirable neutron events may be recorded indistinguishably from γ-rays. Eqs. (22–25) may be used to evaluate the effect of neutron detection on $\langle k\rangle$, σ_k and $\Delta M_\gamma/\langle M_\gamma\rangle$. An approximate value of 0.5 $\Omega_{T,\nu} = N\Omega_\nu$, the total neutron detection efficiency, is estimated on the basis of an inelastic scattering cross-section in iodine of 2 barns and a total scattering cross section for iodine of ~5 barns resulting in an average pulse height of ~0.5 MeV. A reasonable estimate of ~0.2 for F_ν the neutron scattering will be used. As an example of the effect of neutron detection on the multiplicity resolution we show in fig. 11 a plot of $\Delta M_\gamma/\langle M_\gamma\rangle$ versus M_γ for two values of $N = 72$ and 162. In that calculation we assumed $\Omega_T = 0.95$, $E_\gamma = 0.25$, $F_\nu = 0.2$ and a neutron multiplicity $x = 5$. The results for $N\Omega_\nu = 0$ and $N\Omega_\nu = 0.5$ are shown versus M_γ for $N = 72$ and 162. The loss of resolution is very pronounced at low values of M_γ. For heavy-ion induced reactions at incident energies of ~10 MeV amu^{-1} neutron multiplicities as high as 10 have been observed. For those cases the loss of multiplicity resolution would be approximately twice that shown in fig. 11, indicating very poor performance for $M_\gamma \lesssim 20$. These results indicate that identification of the neutron pulses is essential for the performance of the spectrometer for γ-ray multiplicity determinations.

Examples of the response functions for a spectrometer with $N = 72$, $\Omega_T = 0.94$, $F_\gamma = 0.25$, and $N\Omega_\nu = 0.13$ (~72% neutron rejection) were shown in fig. 2.

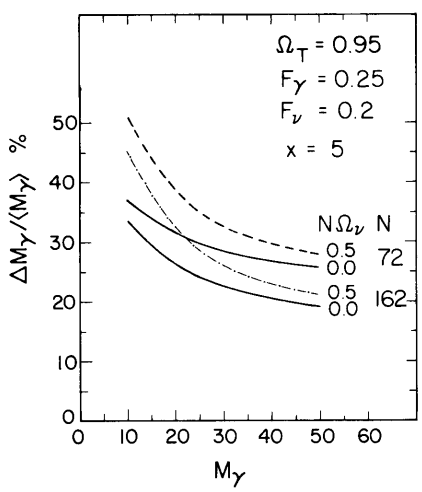

Fig. 11. Effect of neutron detection on the γ-multiplicity resolution for two spectrometers with $N = 72$ and 162. Results are shown for $N\Omega_\nu = 0$ and 0.5, calculated for fixed $\Omega_T = 0.95$, $F_\gamma = 0.25$, $F_\nu = 0.2$ assuming a neutron multiplicity $x = 5$.

3.2. Total pulse-height resolution

The response of the spectrometer for total pulse height is governed by the first few moments of $P_{NHk}(E, M_\gamma)$ with respect to H as given by eqs. (28), (32) and (33). In turn, these moments of H are determined by the spectral functions $\omega_l^{(\alpha)}$ of eq. (27). It is interesting to evaluate $\langle H\rangle$, σ_H and s_H in some simple cases in order to illustrate the performance of the spectrometer in terms of the detection efficiency.

First we point out that from eq. (27)

$$\omega_0^{(\alpha)} = N\sum_\kappa \Omega^{(\alpha)}(h_\kappa) + N(N-1)\sum_{\kappa\lambda} T^{(\alpha)}(h_\kappa h_\lambda) + \ldots$$
$$= \Omega' + \Omega'' + \ldots = \Omega_T^{(\alpha)}\,, \tag{39}$$

which is the total triggering efficiency above some discriminator level. The first spectral function $\omega_1^{(\alpha)}$ determines the response for total pulse height via eqs. (28) and (27). It is possible to define $\Omega_\kappa^{(i)}(E_\gamma)$ and $\Omega_{E_\gamma\kappa}$ to include the scattering to all orders as follows:

$$\omega_0 = \sum_{i=1}^{N}\sum_\kappa \Omega_\kappa^{(i)}(E_\gamma) = \Omega_T\,, \tag{40}$$

$$\omega_1 = \sum_{i=1}^{N}\sum_\kappa \Omega_\kappa^{(i)}(E_\gamma) H_\kappa = \sum_\kappa \Omega_{E_\gamma\kappa} H_\kappa\,, \tag{40a}$$

and

$$\omega_l = \sum_{i=1}^{N}\sum_\kappa \Omega_\kappa^{(i)}(E_\gamma) H_\kappa^l = \sum_\kappa \Omega_{E_\gamma\kappa} H_\kappa^l\,, \tag{40b}$$

where $\Omega_\kappa^{(i)}(E_\gamma)$ and $\Omega_{E_\gamma\kappa}$ can be measured with monoenergetic sources. The former corresponds to the efficiency of the i^{th} detector to record h_κ when the entire spectrometer records pulse height H_κ with efficiency $\Omega_{E_\gamma\kappa}$ from a monoenergetic source of energy E_γ. In contrast $\Omega^{(\gamma)}(h_\kappa)$ in eq. (27) is the efficiency for one detector element in the spectrometer to record h_κ when no other detector records anything. For a given incident energy E_γ it is possible to define average total efficiencies $\bar{\Omega}_{E_\gamma}^{(l)}$ such that

$$\omega_l = \sum_\kappa \Omega_{E_\gamma\kappa} H_\kappa^l = \bar{\Omega}_{E_\gamma}^{(\gamma)} E_\gamma^l\,, \tag{41}$$

and

$$\Omega_T f_{E_\gamma} < \bar{\Omega}_{E_\gamma}^{(l)} < \ldots < \bar{\Omega}_{E_\gamma}^{(1)} < \bar{\Omega}_{E_\gamma}^{(0)} = \Omega_T\,, \tag{41a}$$

where f_{E_γ} is the peak-to-total ratio for E_γ measured

with the complete spectrometer and

$$\lim_{l\to\infty} \bar{\Omega}_{E_\gamma}^{(l)} = f_{E_\gamma}\Omega_T \,. \tag{41b}$$

For values of $f_{E_\gamma}\Omega_T \approx 0.8$–$0.9$ a good approximation is

$$\Omega_{E_\gamma} = \bar{\Omega}_{E_\gamma}^{(1)} \simeq \bar{\Omega}_{E_\gamma}^{(2)} \simeq \bar{\Omega}_{E_\gamma}^{(3)} = f_{E_\gamma}\Omega_T \,. \tag{42}$$

Assuming further M_γ incident γ-rays with E_γ we find from eqs. (28) and (34a)

$$\langle H_\gamma \rangle = M_\gamma \Omega_{E_\gamma} E_\gamma \tag{43}$$

$$\sigma_H = E_\gamma [M_\gamma \Omega_{E_\gamma}(1 - \Omega_{E_\gamma})]^{1/2} \tag{43a}$$

$$\sigma_H(\langle H \rangle = \left(\frac{1 - \Omega_{E_\gamma}}{M_\gamma \Omega_{E_\gamma}}\right)^{1/2} \tag{43b}$$

$$s_H = \frac{1 - 2\Omega_{E_\gamma}}{[M_\gamma \Omega_{E_\gamma}(1 - \Omega_{E_\gamma})]^{1/2}} \tag{43c}$$

which are precisely the moments of the binomial distribution given by eq. (20). If the exact values of ω_l are used somewhat narrower distributions (smaller than $\Delta H/\langle H \rangle$) are obtained compared with those of the binomial distribution, but the values of the skewness s_H are essentially unchanged.

To demonstrate the dependence of the total pulse-height resolution on Ω_{E_γ} and M_γ we plot in fig. 12 the % resolution $\Delta H/\langle H \rangle$ versus M_γ for $\Omega_{E_\gamma} = 0.80$, 0.85 and 0.95. These values were calculated ignoring the effect of neutron detection. It is seen from fig. 12 that the total pulse-height resolution is considerably better than the $\Delta M/\langle M_\gamma \rangle$, at least for values of $\Omega_{E_\gamma} \geqslant 0.8$.

It is possible to estimate the effect of neutron detection on the resolution $\Delta H/\langle H \rangle$ by using eqs. (30), (32) and (32a). For $\Omega_{E_\gamma} = 0.85$ and an assumed neutron multiplicity of $x = 5$ we show in fig. 13 a comparison of the resolutions for total neutron energy detection efficiency $\Omega_{E_\nu} = 0$ and 0.5 as a function of M_γ. As expected considerable loss of resolution occurs at low M_γ values.

3.3. Convenient evaluation of the response functions

In many reaction studies it is desirable to determine the population distributions $Q(E, J)$ or $Q(E, M_\gamma)$ and their projections

$$q(M_\gamma) = \sum_E Q(E, M_\gamma)$$

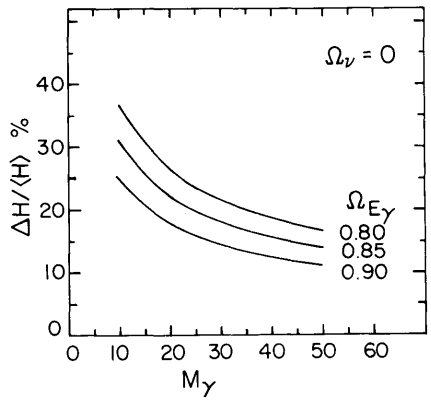

Fig. 12. Dependence of the percent toal pulse-height resolution $\Delta H/\langle H \rangle$ on M_γ for three values of the total energy absorption efficiency Ω_{E_γ} = 0.8, 0.85 and 0.90. Neutron detection was ignored in this case ($\Omega_\nu = 0$).

and

$$q(E) = \sum_{M_\gamma} Q(E, M_\gamma) \,.$$

For this purpose the populations $R(H, k)$ for total-pulse-height H for each fold k must be measured and $Q(E, J)$ must be evaluated from

$$Q(E, M_\gamma) = \sum_{h,k} R(H, k)\, P_{NHk}(E, M_\gamma) \,. \tag{44}$$

Similar expressions for $q(M_\gamma)$ and $q(E)$ may be written as

$$q(M_\gamma) = \sum_k r(k)\, P_{Nk}(E, M_\gamma) \,,$$

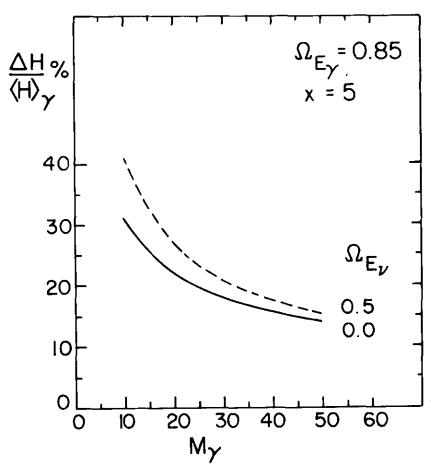

Fig. 13. Effect of neutron detection on the percent total pulse-height resolution as a function of M_γ evaluated for Ω_{E_ν} = 0 and 0.5 assuming constant Ω_{E_γ} = 0.85 and neutron multiplicity x = 5.

and

$$q(E) = \sum_H r(H)\, P_{NH}(E, M_\gamma) ,$$

where $r(k)$ and $r(H)$ are the experimental populations for k and H, respectively.

The precise evaluation of the response $P_{NHk}(E, M_\gamma)$ depends on the input spectrum $\{E_i\}_{I=1,\ldots,M_\gamma}$ of M_γ γ-rays. In the present discussion it will be assumed that the structure of the de-excitation spectrum will be given. This can be the spectrum for an average decay, over the many possible paths for connecting a state at (E, J) with the ground state. A rotational type spectrum with an average moment of inertia and 3–4 additional statistical γ-rays may also be a suitable input. Another less realistic approximation for the decay path may assume M_γ γ-rays of equal, but unknown average γ-ray energy $\bar{E}_\gamma$. It is desirable to give a simple procedure for evaluating $P_{NHk}(E, M_\gamma)$ without making use of the computationally complex expressions (10) and (18a). For this purpose we can use modified gaussian distributions that include properly the first three moments of the exact distribution $P_{NHk}(E, M_\gamma)$ with respect to k, H as well as first order correlation $\langle kH \rangle$.

This procedure for evaluating $P_{NHk}(E, M_\gamma)$ is a generalization of a similar method for evaluating the projections of $P_{NHk}(E, M_\gamma)$ on k or H to give the useful response functions $P_{Nk}(E, M_\gamma)$ and $P_{NH}(E, M_\gamma)$. The procedures for evaluating the latter two response functions will be described next.

3.3.1. A rapid evaluation of $P_{Nk}(E, M_\gamma)$

We note first that the distributions in fold k evaluated via eqs. (10) and (17) for given M_γ and illustrated in fig. 2a can be approximated quite well with gaussian curves with $\langle k \rangle$ and σ_k values obtained via eqs. (22–25). As an example we note that in the average $\bar{\Omega}_\gamma$ approximation ($E = M_\gamma E_\gamma$) with $\bar{\Omega}_\gamma = 0.95/72$, $F_\gamma = 0.25$, $\Omega_v = 0.13/72$ and $M_\gamma = 30$ we find $\langle k \rangle = 28.2825$, $\sigma_k = 2.5945$ and $s_k = 0.0427$. For such small values of the skewness an excellent approximation to the $P_{NK}(E, M_\gamma)$ distribution is given by

$$P_N(k; E, M_\gamma) = \frac{1 + (c_\kappa/3!)\, H_3(\kappa)}{(2\pi)^{1/2}\sigma_\kappa}\, e^{-\kappa^2/2} , \qquad (45)$$

where $\kappa \equiv (k - m_k)/\sigma_\pi$, and the third Hermite polynomial $H_3(\kappa) = 8\kappa^3 - 12\kappa$. The area and the parameters m_k, σ_κ and c_κ for the most probable value, the width and the skewness, are related to the central moments $\mu_{n,k}$ of $P_{Nk}(E, M_\gamma)$ via the expressions

$$\mu_{0,k} = \text{area} = 1 \, , \mu_{1,k} = 0 , \qquad (46)$$

$$\langle k \rangle = m_k + 2\sigma_\kappa c_\kappa , \qquad (46c)$$

$$\mu_{2,k} = \sigma_k^2 = \sigma_\kappa^2(1 - 4c_\kappa^2) , \qquad (46b)$$

$$\mu_{3,k} = 8\sigma_\kappa^3 c_\kappa(1 + 2c_\kappa^2) . \qquad (46c)$$

and

$$s_k = \frac{\mu_3}{\mu_2^{3/2}} = 8c_\kappa \frac{1 + 2c_\kappa^2}{(1 - 4c_\kappa^2)^{3/2}} \simeq 8c_\kappa(1 + 8c_\kappa^2) . \qquad (46d)$$

Thus, to construct $P_N(k; E, M_\gamma)$ we obtain $\langle k \rangle$, σ_k and s_k from eqs. (22a), (23) and (23b). The parameters c_κ, σ_κ and m_k are then calculated from eqs. (46d), (46b) and (46a), respectively. The complete matrix $P_N(k; E, M_\gamma)$ is then evaluated using eq. (45).

3.3.2. A rapid evaluation of $P_{NH}(E, M_\gamma)$

It was mentioned earlier that the true distribution in H has almost the same skewness as that of the binomial distribution [eq. (43c)] but its width is somewhat smaller. Again an expression of the form of eq. (45) is a good representation of the $P_{NH}(E, M_\gamma)$ distribution. Thus,

$$P_N(H; E, M_\gamma) = \frac{1 + (c_\eta/3!)\, H_3(\eta)}{\sigma_\eta(2\pi)^{1/2}}\, e^{-\eta^2/2} , \qquad (47)$$

where $\eta = (H - m_H)/\sigma_\eta$ and m_H, σ_η and c_η are given by

$$\mu_{0,H} = 1, \mu_{1,H} = 0 , \qquad (48)$$

$$\langle H \rangle = m_H + 2\sigma_\eta c_\eta , \qquad (48a)$$

$$\mu_{2,H} = \sigma_H^2 = \sigma_\eta^2(1 - 4c_\eta^2) , \qquad (48b)$$

$$\mu_{3,H} = 8\sigma_\eta^3 c_\eta(1 + 2c_\eta^2) , \qquad (48c)$$

and

$$s_H = \frac{\mu_{3,H}}{\sigma_H^3} = 8c_\eta \frac{1 + 2c_\eta^2}{(1 - 4c_\eta^2)^{3/2}} \simeq 8c_\eta(1 + 8c_\eta^2) . \qquad (48d)$$

The same procedure as in section 3.3.1 is employed to evaluate the matrix $P_N(H; E, M_\gamma)$. The central moments with respect to H are evaluated via eqs. (28), (32) and (33). The parameters m_H, σ_η and c_η are then evaluated from eqs. (48a), (48b) and (48d).

3.3.3. The bivariate distribution $P_{NHk}(E, M_\gamma)$

It should be recognized that for given (E, M_γ) the distribution in (H, k) is a bivariate distribution of the closely correlated variables H and k. This distribution, however, deviates slightly from a normal

bivariate distribution since the third and higher moments, although small, are non-zero. Again we shall approximate the deviation from the normal distribution by incorporating the knowledge of the third moment. We can write for the skewed bivariate distribution function:

$$P_N(Hk; E, M_\gamma) = \frac{[1 + (c_\kappa/3!)\,H_3(\kappa)]\,[1 + (c_\eta/3!)\,H_3(\xi)]}{2\pi\sigma_\eta\sigma_\kappa(1-\rho^2)^{1/2}} \times e^{-\xi^2/2} e^{-\kappa^2/2} \tag{49}$$

$$= \frac{[1 + (c_\eta/3!)\,H_3(\eta)]\,[1 + (c_\kappa/3!)\,H_3(\zeta)]}{2\pi\sigma_\eta\sigma_\kappa(1-\rho^2)^{1/2}} \times e^{-\zeta^2/2} e^{-\eta^2/2} \tag{49a}$$

where

$$\kappa \equiv (k - m_k)/\sigma_\kappa\,, \qquad \eta \equiv (H - m_H)/\sigma_\eta\,, \tag{50}$$

$$\xi \equiv \frac{\eta - \rho\kappa}{(1-\rho^2)^{1/2}}, \qquad \zeta \equiv \frac{\kappa - \rho\eta}{(1-\rho^2)^{1/2}} \tag{50a}$$

$$\rho = \langle Hk\rangle/\langle H\rangle\langle k\rangle\,, \tag{50b}$$

$$\langle k\rangle = m_k + 2\sigma_\kappa c_\kappa\,, \tag{50c}$$

$$\sigma_k^2 = \sigma_\kappa^2(1 - 4c_\kappa^2)\,, \tag{50d}$$

$$s_k = 8c_\kappa(1 + 8c_\kappa^2)\,, \tag{50e}$$

$$\langle H\rangle = m_H + 2\sigma_\eta\sigma_\eta\,, \tag{50f}$$

$$\sigma_H^2 = \sigma_\eta^2(1 - 4c_\eta^2)\,, \tag{50g}$$

$$s_H = 8c_\eta(1 + 8c_\eta^2)\,, \tag{50h}$$

and

$$\int_0^\infty P_N(Hk; E, M_\gamma)\,\mathrm{d}H = \frac{1 + (c_\kappa/3!)\,H_3(\kappa)}{(2\pi)^{1/2}\sigma_\kappa}\, e^{-\kappa^2/2}\,, \tag{51}$$

$$\int_0^\infty P_N(Hk; E, M_\gamma)\,\mathrm{d}k = \frac{1 + (c_\eta/3!)\,H_3(\eta)}{(2\pi)^{1/2}\sigma_\eta} \times e^{-\eta/2}\,, \tag{51a}$$

$$\int_0^\infty\int_0^\infty P_N(Hk; E, M_\gamma)\,\mathrm{d}H\,\mathrm{d}k = 1\,. \tag{51b}$$

It is clear from eq. (49) that the most probable value occurs for $\eta = \kappa = 0$, but the ridge of most probable values is determined by $\eta = \rho\kappa$ and its amplitude is modulated by

$$[1 + (c_\kappa/3!)\,H_3(\kappa)]\; \mathrm{e}^{-\kappa^2/2}\,.$$

For problems of interest here eq. (38) gives $0.96 \lesssim \rho < 1$. However, values of $\rho \simeq 0.99$ would be common if the effect of the interfering neutrons is reduced to ~1/10. This indicates a strong correlation between H and k. Thus, for fixed κ (given fold k) the width of the distribution in η (distribution in H) is reduced to $\sigma_H(1-\rho^2)^{1/2}$. Similarly, for fixed η (given H) the width of the distribution in κ is reduced to $\sigma_k(1-\rho^2)^{1/2}$.

We wish to thank M.L. Halbert, J.H. Barker and H. Jääskeläinen for valuable discussions.

Appendix A

The probabilities $P_{NH}(n_1,..., n_N)$ are generated [eq. (5)] by $G(t,..., t; s_1,..., s_n)$ and hence $F(t, s)$ [eq. (7)] can be expressed in terms of $G(t,..., t; s_1,..., s_n)$. In fact

$$P_{NH}(n_1 \ldots n_N) = \left(\frac{1}{2\pi i}\right)^{N+1} \oint \frac{\mathrm{d}\tilde{t}}{\tilde{t}^{H+1}} \oint \frac{\mathrm{d}s_1}{s_1^{n_1+1}} \ldots \oint \frac{\mathrm{d}s_N}{s_N^{n_N+1}}\, G(\tilde{t},..., \tilde{t}; s_1,..., s_N)$$

with all contours encircling the origin. $G(\tilde{t},..., \tilde{t}; s_1,..., s_N)$ itself has no singularities for finite arguments. Thus

$$F(t, s) = \sum_{H=0}^{\infty} t^H \sum_{n_1 \ldots n_N} s^{N - \delta^0_{n(1)} - \ldots - \delta^0_{n(N)}} \times \left(\frac{1}{2\pi i}\right)^{N+1} \oint \frac{\mathrm{d}\tilde{t}}{\tilde{t}^{H+1}} \oint \frac{\mathrm{d}s_1}{s_1^{n_1+1}} \ldots \oint \frac{\mathrm{d}s_N}{s_N^{n_N+1}} \times G(\tilde{t},..., \tilde{t}; s_1,..., s_N)\,.$$

If the contours maintain $|\tilde{t}| > |t|$ and $|s_i| > |s|$, the sums may be performed first to give

$$F(t, s) = \left(\frac{1}{2\pi i}\right)^{N+1} \oint \frac{\mathrm{d}\tilde{t}}{\tilde{t} - t} \oint \mathrm{d}s_1 \left(\frac{1-s}{s_1} + \frac{s}{s_1 - 1}\right) \ldots \oint \mathrm{d}s_N \left(\frac{1-s}{s_N} + \frac{s}{s_N - 1}\right) G(\tilde{t},..., \tilde{t}; s_1,..., s_N)\,.$$

The contours include the singularities at $\tilde{t} = t$, $s_i = 0$ and $s_i = 1$ so

$$F(t, s) = \sum_{i_1=0,1} (1-s)^{1-i_1} s^{i_1} \ldots \sum_{i_N=0,1} (1-s)^{1-i_N} s^{i_N}$$

$$\times G(t,\ldots,t;i_1,\ldots,i_N)$$

$$= \sum_{0\leqslant i_1\ldots i_N\leqslant 1} (1-s)^{N-i_1\ldots-i_N} s^{i_1+\ldots+i_N}$$

$$\times G(t,\ldots,t;i_1,\ldots,i_N)$$

$$= \sum_{n=0} (1-s)^{N-n}s^n \sum_{\substack{0\leqslant i_1\ldots i_N\leqslant 1\\ i_1+\ldots+i_N=n}} G(t,\ldots,t;i_1,\ldots,i_N)$$

which is eq. (8).

Appendix B

All of the N-dependence in eq. (37a) is explicit. The following transformation makes it possible to perform the sum over n. After this the $N\to\infty$ limit is straightforward. The bracketed expression in eq. (37a) is a second order polynomial in n and may be factored

$$1-\frac{N-n}{N}\left[\Omega'+\Omega''\frac{N+n-i}{N-i}\right]$$

$$=\frac{1-\Omega'-\Omega''}{N^2x_1x_2}(n-Nx_1)(n-Nx_2)\,.$$

The zeros Nx_1, Nx_2 are functions of Ω', Ω'' and N. In terms of an expansion in $1/N$, $x_i = x_i^0 + 0(1/N)$, $i=1,2$, with

$$\left.\begin{matrix}x_1^0\\ x_2^0\end{matrix}\right\} = \frac{-\Omega' \pm [\Omega'^2 - 4\Omega''(1-\Omega'-\Omega'')]^{1/2}}{2\Omega''}\,.$$

Consider

$$F_{M_1M_2}(s) = \left(\frac{1-\Omega'-\Omega''}{x_1x_2}\right)^{M_\gamma}\sum_{n=0}^{N} s^n(1-s)^{N-n}\binom{N}{n}$$

$$\times\left(\frac{n}{N}-x_1\right)^{M_1}\left(\frac{n}{N}-x_2\right)^{M_2}\,.$$

When $M_1=M_2=M_\gamma$, this reduces to $F(s)$ of eq. (37a). Now

$$\sum_{M_1,M_2=0}^{\infty}\frac{\mu_1^{M_1}\mu_2^{M_2}}{M_1!M_2!}F_{M_1M_2}(s) = \left(\frac{1-\Omega'-\Omega''}{x_1x_2}\right)^{M_\gamma}$$

$$\times\sum_{n=0}^{N} s^n(1-s)^{N-n}$$

$$\times\binom{N}{n}\exp\left[\mu_1\left(\frac{n}{N}-x_1\right)+\mu_2\left(\frac{n}{N}-x_2\right)\right]$$

$$=\left(\frac{1-\Omega'-\Omega''}{x_1x_2}\right)^{M_\gamma}e^{-\mu_1x_1-\mu_2x_2}$$

$$\times(1-s+se^{(\mu_1+\mu_2)/N})^N\,.$$

Each factor in this expression has a limit as $N\to\infty$. Thus

$$\sum_{M_1M_2=0}^{\infty}\frac{\mu_1^{M_1}}{M_1!}\frac{\mu_2^{M_2}}{M_2!}\lim_{N\to\infty}F_{M_1M_2}(s)$$

$$=\left(\frac{1-\Omega'-\Omega''}{x_1^2x_2^0}\right)^{M_j}e^{-\mu_1x_1^0-\mu_2x_2^0}e^{s(\mu_1+\mu_2)}$$

and

$$\lim_{N\to\infty}F_{M_1M_2}(s) = \left(\frac{1-\Omega'-\Omega''}{x_1^0x_2^0}\right)^{M_\gamma}(s-x_1^0)^{M_1}$$

$$\times(s-x_2^0)^{M_2}\,.$$

$M_1=M_2=M_\gamma$ recovers

$$\lim_{N\to\infty}F(s)=\left[\frac{1}{4\Omega''}\left(s^2+\frac{\Omega'}{\Omega''}s+4\Omega''(1-\Omega'-\Omega'')\right)\right]^{M_\gamma}.$$

Expanding in s gives eq. (37b).

References

[1] G.B. Hagemann, R. Broda, B. Herskind, M. Ishihara, S. Ogaza and H. Ryde, Nucl. Phys. A245 (1975) 166.

[2] D.G. Sarantites, J.H. Barker, M.L. Halbert, D.C. Hensley, R.A. Dayras, E. Eichler, N.R. Johnson and S. Gronemeyer, Phys. Rev. C14 (1976) 2138.

[3] L. Westerberg, D.G. Sarantites, R. Lovett, J.T. Hood, J.H. Barker, C.M. Currie and N. Mullani, Nucl. Instr. and Meth. 145 (1977) 295.

[4] D.G. Sarantites, L. Westerberg, R.A. Dayras, M.L. Halbert, D.C. Hensley and J.H. Barker, Phys. Rev. C17 (1978) 601.

[5] D.G. Sarantites, L. Westerberg, M.L. Halbert, R.A. Dayras, D.C. Hensley and J.H. Barker, Phys. Rev. C18 (1978) 774.

[6] L. Westerberg, D.G. Sarantites, D.C. Hensley, R.A. Dayras, M.L. Halbert and J.H. Barker, Phys. Rev. C18 (1978) 796.

[7] J.O. Newton, J.C. Lisle, G.D. Dracoulis, J.R. Leigh and D.C. Weissner, Phys. Rev. Lett. 34 (1975) 99.

[8] M.V. Banaschik, R.S. Simon, P. Colombani, D.P. Soroka and F.S. Stephens, Phys. Rev. Lett. 34 (1975) 892.

[9] R.S. Simon, M.V. Ban a schik, P.Colombani, D.P. Soroka, F.S. Stephens and R.M. Diamond, Phys. Rev. Lett. 36 (1976) 359.

[10] F.J. Feenstra, et al., Phys. Lett. 69B (1977) 403.

[11] L. Westerberg, D.G. Sarantites, K. Geoffroy, R.A. Dayras, J.R. Beene, M.L. Halbert, D.C. Hensley and J.H. Barker, Phys. Rev. Lett. 41 (1978) 96.

[12] T.D. Khoo, R.K. Smither, B. Haas, O. Hausser, H.R. Andrews, D. Horn and D. Ward, Phys. Rev. Lett. 41 (1978) 1027.

[13] R. Woodward and D.G. Sarantites, to be published.